



Impact of large-scale magnetic particle synthesis on nucleic acid extraction consistency and efficiency

Petra Stejskalová ^a, Martin Ženka ^b, Zbyněk Šplíchal ^a, Pavel Švec ^a, Jiří Kudr ^a, Eva Jansová ^a, Miloš Dendis ^b, Ondřej Zítka ^{a,c,*}

^a Department of Chemistry & Biochemistry, Mendel University in Brno, Zemědělská 1, Brno 61300, Czech Republic

^b GeneProof, Vídeňská 101/119, Brno 619 00, Czech Republic

^c Department of Microelectronics, Faculty of Electrical Engineering and Communication Technology, Brno University of Technology, Technická 10, Brno 61600, Czech Republic

ARTICLE INFO

Keywords:
Nanoparticles
Silica
Hydrated
Lyophilized
CMV
HCV

ABSTRACT

Nucleic acids (NAs) extraction is a critical step in molecular biology. Traditional methods, such as phenol-chloroform extraction and spin-column purification, present automation and scalability limitations. In this study, we present the synthesis, scale-up, characterization, and application of MPs for the automated NAs extraction from HCV and CMV. These pathogens are routinely included in high-throughput screening assays, underscoring the necessity for automated NAs isolation processes. We scaled the synthesis from 1 L to 5 L batch volumes, yielding MPs with consistent physicochemical properties and an average particle diameter of 44.72–46.57 nm. Larger-scale MPs maintained extraction efficiency with minimal Ct variation (≤ 1.0) across replicates. Compared to commercial alternatives, our hydrated MPs demonstrated over 5 % improvement in DNA extraction efficiency, though RNA recovery exhibited higher variability. Additionally, we investigated the stability and storage conditions of MPs in hydrated and lyophilized forms. Hydrated MPs consistently outperformed lyophilized counterparts, showing up to a 3.5 Ct lower value in DNA extraction, corresponding to a higher than 1-log increase in extraction efficiency. This study demonstrates the successful scale-up of TEOS modified MPs while maintaining batch-to-batch consistency and long-term stability over two years. The developed MPs offer a robust, cost-effective, and efficient platform for automated NAs extraction, with potential for integration into molecular diagnostics, high-throughput workflows, and point-of-care diagnostic tools, particularly in decentralized or resource-limited settings.

1. Introduction

Nucleic acids (NAs) extraction is a fundamental procedure in the field of molecular biology and diagnostics, underpinning a wide range of applications from genetic research to clinical testing. The fast isolation of high-purity and integrity NAs from diverse biological matrices is a prerequisite for the analytical precision, sensitivity, and reproducibility of downstream molecular assays, including polymerase chain reaction (PCR), loop-mediated isothermal amplification (LAMP), next-generation sequencing (NGS), and microarray-based platforms, especially when processing complex samples that contain inhibitors or samples with low concentrations of target NA [1–4]. In clinical practice, the effective isolation of NA enables pathogen detection, mutation analysis, and gene expression profiling, all of which are crucial for patient diagnosis,

prognosis, and treatment [5–7]. Several methods have been developed for NA extraction, primarily categorized into two main approaches: fluid-phase and solid-phase methods [8–10]. The choice of method depends on the type of biological sample, required purity, and downstream application. Fluid-phase methods, such as phenol-chloroform extraction, use organic solvents for separation but often require optimization and may co-purify PCR inhibitors [8,11,12]. Solid-phase methods, such as silica spin column-based extraction, enable NA binding under high-salt conditions followed by washing and elution steps [13–15]. Despite their effectiveness, these methods are generally unsuitable for automation and are labor-intensive, limiting their scalability for high-throughput applications [16–19].

In recent years, magnetic particles (MPs) have been established as a highly efficient, versatile, and automation-compatible alternative for NA

* Corresponding author at: Department of Chemistry & Biochemistry, Mendel University in Brno, Zemědělská 1, Brno 61300, Czech Republic.
E-mail address: ondrej.zitka@mendelu.cz (O. Zítka).

extraction, which has significantly impacted molecular diagnostics [20–23]. The use of MPs facilitates streamlined sample processing, ensuring high purity and yield [24,25]. This significantly increases diagnostic accuracy and reduces turnaround times [26,27]. The surface of MPs is typically functionalized with specific chemical groups that provide selective and efficient adsorption of NA from complex biological samples in the presence of chaotropic salts [28,29]. This allows other molecules and contaminants to be removed during the washing process [30]. Compared to spin column methods, MPs-based NA extraction is particularly suitable for integration into microfluidic or automated platforms. This facilitates consistent, high-throughput sample processing with minimal manual effort. Despite these advantages, RNA extraction presents distinct challenges. Compared to DNA, RNA is structurally less stable and more susceptible to degradation by ubiquitous RNases [31,32]. Moreover, its single-stranded nature and secondary structure can interfere with efficient binding to MPs, especially if the surface chemistry is not optimized. Many MPs formulations exhibit reduced RNA recovery, particularly at low copy numbers or when handling degraded clinical specimens [33,34]. These limitations underscore the need for extraction platforms that are equally effective for both DNA and RNA, especially in multiplex diagnostic assays. Although MPs have demonstrated clear advantages in NA extraction, scaling their production for commercial use poses considerable challenges. Producing MPs with appropriate surface chemistry, uniform properties, and stable performance for reliable NA isolation is technically demanding, particularly as production batch sizes increase [35]. Commercial synthesis must effectively manage size distribution, particle aggregation, and functionalization efficiency to ensure that each batch meets strict quality and performance standards [36]. Achieving scalability and reproducibility at larger production volumes is a critical challenge, especially as the demand for high-quality MPs grows in research and clinical laboratories worldwide [37].

In this work, we synthesized and characterized tetraethyl orthosilicate (TEOS) modified MPs and evaluated their efficiency in automated NA extraction. We investigated the scalability of MPs production by comparing batches synthesized at different volumes and assessed their stability over long-term storage. Additionally, we examined the impact of MPs' physical state (hydrated vs. lyophilized) on NA extraction efficiency. Our findings provide insights into the reproducibility and robustness of MPs for large-scale applications and highlight key factors influencing their performance in molecular diagnostics.

2. Materials and methods

2.1. Chemicals

$\text{FeSO}_4 \cdot 7 \text{H}_2\text{O}$, KNO_3 , H_2SO_4 (95–98 %), TEOS, and other chemicals were purchased from Sigma-Aldrich (St. Louis, MO, USA) in ACS purity and were used as received. Potassium hydroxide (1 M) was ordered from Supelco (Bellefonte, PA, USA). The plasma used in this study was sourced from The University Hospital Brno (Czech Republic) and served as the clinical material. All plasma samples were collected from healthy donors and were confirmed to be negative for the viruses being investigated. NA extraction was performed using the myCROBE/croBEE 2.0 Universal Extraction Kit purchased from GeneProof (Brno, Czech Republic). Additionally, the myCROBE Universal Internal Control (UNIC) from GeneProof (Brno, Czech Republic) was employed to verify the extraction process. All water-based solutions were prepared using milli-Q water (resistivity higher than $18.2 \text{ M}\Omega \cdot \text{cm}$ at 25°C) from Millipore unless stated otherwise (Burlington, MA, USA).

2.2. Magnetic particles synthesis

Magnetic particles were synthesized using the modified method based on the approach proposed by Sugimoto and Matijevic [38]. Specifically, 34.8 g of $\text{FeSO}_4 \cdot 7 \text{H}_2\text{O}$ was dissolved within 150 mL of water

with the addition of 15 μL of sulfuric acid. The solution was subsequently degassed. In a separate 5 L reagent flask, 4.3 L of mQ water, 101.1 g of KNO_3 , and 500 mL of 1 M KOH were added, and this solution was degassed. Both solutions were mixed in a reagent flask, covered with a cap, and placed in a water bath preheated to 90°C , where they were kept for 3 h. The obtained magnetic solid was thoroughly washed using a permanent magnet. Subsequently, particles were dispersed in 1 L of 0.5 M sodium citrate water solution and incubated in a water bath at 80°C for 1 h. Afterward, the magnetic cores were washed thoroughly using a permanent magnet and prepared for further modification.

2.3. Surface modification of MPs with SiO_2 layer

The magnetic cores were modified with a SiO_2 layer using a modified Stöber method. In this process, the ethoxy groups of TEOS are hydrolyzed in a mixture of distilled water and ethanol in the presence of ammonia as a reaction catalyst. Specifically, using sonication, 4 g of magnetic cores (dry solid) were dispersed in a mixture of 700 mL of water, 1000 mL of pure ethanol, and 51 mL of ammonium hydroxide. The solution was stirred using an overhead stirrer, and 20 mL of TEOS was added gradually. The solution was stirred for 20 h. The resulting material, denoted as MPs-SiO_2 , was washed with ethanol and water using a magnet and then dispersed within the water. The concentration of MPs-SiO_2 was determined by weighing the dry solid of an aliquot.

2.4. MPs preparation for testing in lyophilized and hydrated forms

The hydrated MPs were stored in water, and $1 \text{ mg} \cdot \text{mL}^{-1}$ aliquots were prepared for testing. While preparing the test cartridges, water was removed from the MPs using a magnet. The MPs were then dispersed in a binding buffer from the myCROBE/croBEE 2.0 Universal Extraction Kit (GeneProof, Brno, Czech Republic) at a concentration of $1 \text{ mg} \cdot \text{mL}^{-1}$. These were placed in isolation cartridges and stored for one month before testing. The MPs intended for testing in lyophilized form were frozen using liquid nitrogen at -80°C and subsequently freeze-dried with a FreeZone Benchtop Freeze Dryer (Labconco, Kansas City, MO, USA) at -50°C for 48 h. After lyophilization, 1 mg of aliquots were prepared and stored in microtubes. One month before testing, the lyophilized MPs were dispersed in a binding buffer to a concentration of $1 \text{ mg} \cdot \text{mL}^{-1}$, similar to the hydrated MPs.

2.5. Microscopic analysis and energy-dispersive X-ray spectroscopy

Scanning electron microscopy (SEM) images of MPs were taken on MIRA 2 SEM from TESCAN company (Brno, Czech Republic) using UH resolution mode. Micrographs were obtained using the In-Beam SE detector at 3 mm working distance and 15 kV acceleration voltage. The measurement was performed at a high vacuum. Elements analysis was made on Energy Dispersive Spectroscopy (EDX) detector X-MAX 50 (Oxford Instruments plc, Abingdon, UK) with the same conditions as photos (high vacuum, accelerating voltage 15 kV). Only the work distance was different (15 mm) and the E-T SE detector was used. The power of the detector was set so that the input signal was about 19,000–21,000 cts. At this setting, the output signal was about 15,000–16,000 cts, and detector deadtime fluctuated between 19–21 %. The time for each analysis was 20 min. The spot size was 29 nm.

2.6. Zeta potential analysis assessment by ELS

Particle zeta potential was determined using the electrophoretic light scattering (ELS) method by Zetasizer Nano-ZS (Malvern Instruments Ltd., Worcestershire, UK) with a scattering angle $\theta = 173^\circ$. Samples were analyzed in 10 mM KCl solution.

2.7. Sample preparation for PCR detection of CMV and HCV

Positive samples were prepared by adding Cytomegalovirus (CMV) reference material (WHO/NIBSC 09/162) and Hepatitis C (HCV) S-panel (AcroMetrix™, Thermo Fisher Scientific, Waltham, USA) to plasma samples. The positive samples included CMV in the form of viral DNA and HCV in the form of viral RNA. For the high-positive sample, the CMV concentration was $10,000 \text{ IU} \cdot \text{mL}^{-1}$, while it was $1000 \text{ IU} \cdot \text{mL}^{-1}$ for the low-positive sample. Similarly, the HCV concentration was $10,000 \text{ IU} \cdot \text{mL}^{-1}$ for the high-positive sample and $500 \text{ IU} \cdot \text{mL}^{-1}$ for the low-positive sample. For the HCV, the detection limit is $150 \text{ IU} \cdot \text{mL}^{-1}$. To ensure successful isolation, a threshold of three times the detection limit is used. This guarantees the complete isolation of the pathogen, minimizing the risk of failure due to an insufficient pathogen concentration. Similarly, for CMV, the detection limit is $300 \text{ IU} \cdot \text{mL}^{-1}$. Each concentration of the samples was prepared in triplicate. Both sample types included myCROBE UNIC (Universal Internal Control), containing plasmid DNA for CMV and viral RNA, represented by CDV (*Canine distemper virus*), for HCV. The negative samples consisted solely of plasma with UNIC, without the presence of detectable pathogens.

2.8. Cartridge preparation and automated NA extraction using MPs

The extraction cartridge containing tested MPs was prepared using a standard myCROBE/croBEE 2.0 Universal Extraction Kit cartridge obtained from GeneProof (Brno, Czech Republic). The NA extraction procedure was automatically carried out using the myCROBE® instrument purchased from the same company. The cartridge was sequentially loaded with buffers designed for nucleic acid isolation in the following order: lysis buffer, binding buffer, wash buffer 1, wash buffer 2, wash buffer 3, and elution buffer. The composition of the individual extraction solutions is protected under patent law. $25 \mu\text{L}$ of MPs in $1 \text{ mg} \cdot \text{mL}^{-1}$ content were mixed with $1575 \mu\text{L}$ of binding buffer. First, the sample was combined with $500 \mu\text{L}$ of lysis buffer in the first position of the cartridge and then transferred to the binding buffer with MPs. In the following steps, the MPs-NA complex was washed with $1000 \mu\text{L}$ of wash buffer 1, followed by $1000 \mu\text{L}$ of wash buffer 2, and $1000 \mu\text{L}$ of wash buffer 3. In the final step, the sample was agitated in $200 \mu\text{L}$ of elution buffer to elute the NAs. The myCROBE/croBEE 2.0 Universal Extraction Kit, which included the original MPs, served as a reference.

2.9. Detection of CMV and HCV using RT-qPCR analysis

The GeneProof® Cytomegalovirus (CMV) PCR Kit – (IVDR) (CMV/GP/025) purchased from GeneProof (Brno, Czech Republic) was used for the detection of CMV. The commercial kit includes specific primers targeting a conserved region of UL123, which encodes the immediate-early 1 (IE1) protein. For the detection of HCV, the GeneProof HCVD Diagnostic PCR Kit (HCVD/ISEX/025) was used, utilizing primers designed for the 5' untranslated region (UTR). Each reaction consisted of $30 \mu\text{L}$ of master mix containing PCR enzymes, TaqMan probes, and primers, mixed with $10 \mu\text{L}$ of extracted NA. The extracted NA was replaced with UltraPure™ DNase/RNase-Free Distilled Water (Thermo Fisher Scientific, Waltham, USA) for the negative control. RT-qPCR analysis was performed using the croBEETM Real-Time PCR System (GeneProof, Czech Republic) under the following conditions for HCV detection: reverse transcription at 42°C for 15 min, followed by an initial denaturation at 95°C for 10 min. This was followed by 45 cycles of denaturation at 95°C for 5 s, annealing at 60°C for 40 s, and extension at 72°C for 20 s. For CMV detection, the reaction followed the same setup, excluding the reverse transcription step.

2.10. RT-qPCR results analysis: sensitivity and robustness evaluation

Two fluorescence detection channels, FAM and HEX, were utilized for assessment. The FAM channel detected CMV and HCV. In contrast,

the HEX channel detected plasmid DNA and the CDV viral RNA, both contained within the myCROBE UNIC. Two parameters were evaluated as a result of the testing: sensitivity and robustness. Sensitivity was assessed in the FAM channel by determining the ability of the MPs to achieve positive detection at the same or a higher number of replicates compared to the control magnetic particles included in the myCROBE/croBEE 2.0 Universal Extraction Kit. For all positive samples containing both CMV and HCV, detection in the FAM channel was required to be positive across all three replicates. Robustness was evaluated in the HEX channel based on the consistency of positive detection of myCROBE UNIC plasmid DNA. For all negative internal control (UNIC) samples, detection must be positive in the HEX channel in all three replicates. Robustness was assessed exclusively in negative control samples, as it was not considered a critical parameter for positive samples and was therefore not analyzed for those cases.

2.11. Statistical analysis of RT-qPCR data

The threshold cycles are shown in the graph as the mean \pm standard deviation from three independent replicates. Statistical analysis of the Ct values was conducted using one-way ANOVA, followed by Tukey's multiple comparisons test, employing GraphPad Prism version 8.0.1 (GraphPad Software, CA, USA). A t-test was also performed to identify significant differences between the Ct values. A p-value of less than 0.05 was considered statistically significant.

3. Results and discussion

3.1. Magnetic particles and their properties

In the initial phase, magnetite (Fe_3O_4) MPs cores were synthesized using the method developed by Sugimoto and Matijevic [28], which involves aging $\text{Fe}(\text{OH})_2$ gel at elevated temperatures. This approach allows for control over the morphology of the obtained magnetic material by adjusting parameters including temperature, pH, ions concentration in the solution, and the type of oxidant used. We scaled up the process to produce modified MPs in gram quantities.

The efficiency of NA extraction using MPs is highly dependent on their physicochemical characteristics, including particle size, surface chemistry, magnetic properties, and colloidal stability. The cores produced in various batch sizes, following the procedure outlined in the *Materials and Methods* section, are shown in Fig. 1ABCD. SEM micrographs reveal that the cores exhibit relatively good homogeneity (Fig. 1 IJKL). No unwanted antiferromagnetic $\alpha\text{-FeOOH}$ (goethite) or $\gamma\text{-FeOOH}$ (lepidocrocite), which would be observed as acicular or twinned particles, were observed [39]. The surface of particles was modified with a SiO_2 layer using the Stöber method [40]. In this process, TEOS was hydrolyzed in a mixture of ethanol and water, with ammonia serving as a catalyst. This reaction facilitated the condensation of TEOS on the surface of the MPs, resulting in the formation of a compact SiO_2 layer [41]. SEM images of modified particles from 1 L and 5 L synthesis batches (Fig. 1EFGH) indicate an increase in particle size compared to the MPs core, along with the rounding of previously sharp edges. The slight distortion observed in the SEM image of the TEOS modified MPs is attributed to the insulating, non-conductive nature of the silica coating, which induces sample charging during imaging. High-quality images could not be obtained without sputter-coating the samples with a conductive layer. The particle size distribution of modified MPs was analyzed manually from SEM micrographs ($n = 350$). Results indicate a consistent particle size when scaling up the synthesis of MPs from a 1 to a 5 L volume. MPs synthesized in a 1 L volume exhibited an average size of $46.59 \pm 10.49 \text{ nm}$ (Fig. 1I), while the average size of MPs synthesized in a 5 L volume, based on three independent batches, was 44.72 nm . MPs with smaller sizes and higher surface-to-volume ratios typically provide more binding sites for NA, enhancing overall extraction yield. However, agglomeration or sedimentation which is often influenced by surface

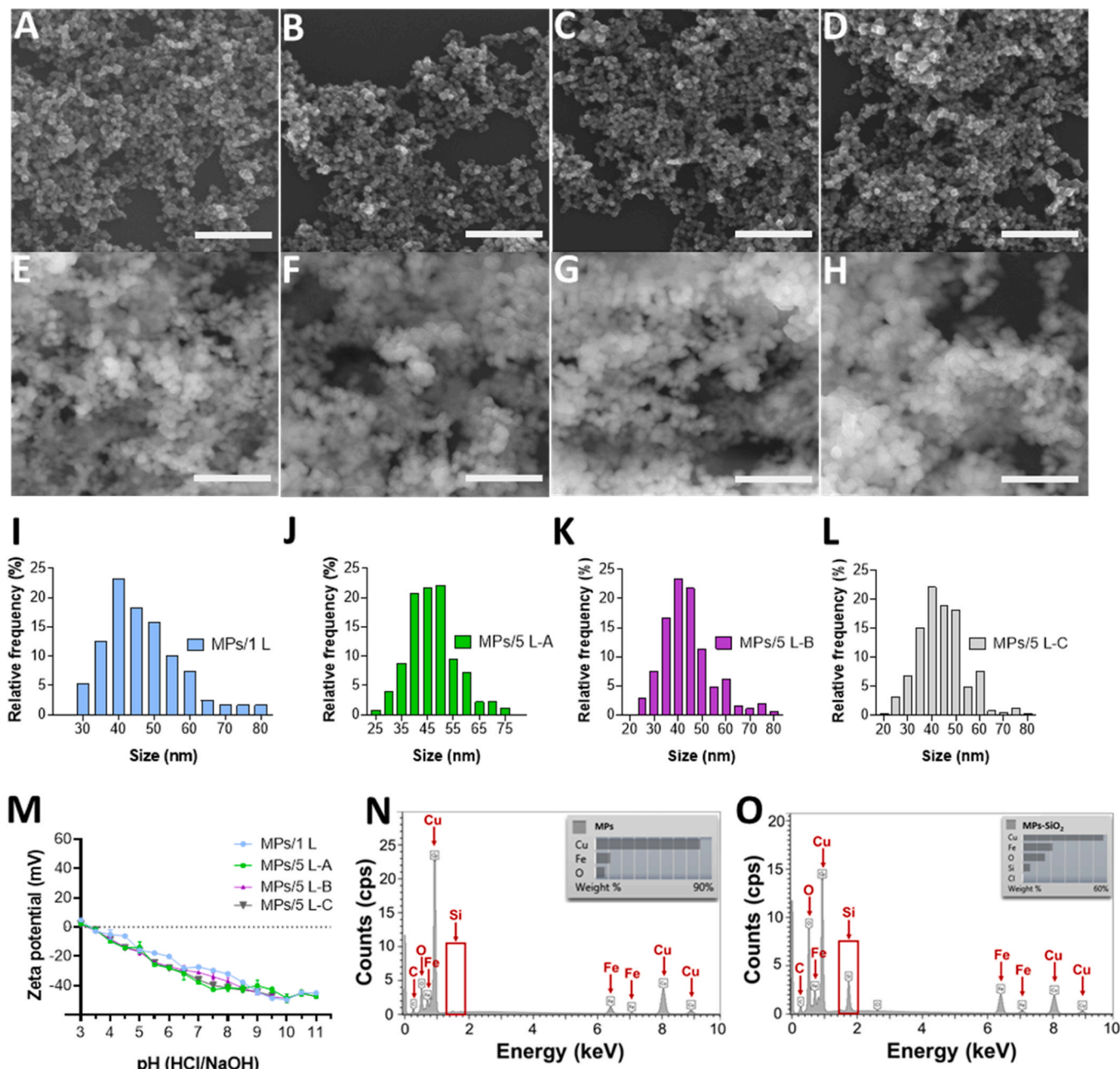


Fig. 1. SEM micrograph of MP cores of individual batches: MP/1 L (A), MP/5 L-A (B), MP/5 L-B (C), and MP/5 L-C (D). SEM micrographs of surface modified MP: MP/1 L (E), MP/5 L-A (F), MP/5 L-B (G), and MP/5 L-C (H) (scale bar: 500 nm). Size distribution of surface modified MP: MP/1 L (I), MP/5 L-A (J), MP/5 L-B (K), and MP/5 L-C (L). (M) Dependence of MP zeta potentials on pH (3–11) of 10 mM KCl solution. EDX spectrum of MP cores (N) and MP modified with SiO₂ layer (O).

charge and dispersibility, can reduce accessibility of binding sites and hinder extraction performance. Size distribution analysis further confirmed consistency across three independent batches of MP synthesized in a 5 L volume, highlighting the reproducibility crucial for industrial applications. The average sizes of MP in batches MP/5 L-A, MP/5 L-B, and MP/5 L-C were 46.57 ± 8.98 nm (Fig. 1J), 43.71 ± 10.16 nm (Fig. 1K), and 43.87 ± 9.62 nm (Fig. 1L), respectively. It represents a decent result for nanoparticles fabricated by the coprecipitation method in such a reaction volume. The zeta potential of four batches of MP modified with a SiO₂ layer was evaluated over a pH range of 3–11 (Fig. 1M). At pH 3, the zeta potential is near zero and follows a similar trend across all batches. The MP exhibit an isoelectric point (IEP) at pH 3.3, where protonated and deprotonated silanol groups are expected to be balanced. At pH > 3.3, deprotonated (negatively

charged) silanol groups dominate, leading to an increasingly negative zeta potential with rising pH. This trend is consistent with the zeta potential behavior of SiO₂ particles [42]. The functional groups present on the MP primarily mediate hydrophobic interactions with the negatively charged phosphate backbone of DNA or RNA [22]. The nature, density, and orientation of these groups critically affect the binding affinity and selectivity toward nucleic acids. Modifications aimed at optimizing surface functionality can significantly improve RNA or DNA recovery, particularly under varying ionic strength and pH conditions encountered in different sample types. The elemental composition of MP cores and SiO₂ modified MP was analyzed using the EDX module of SEM. The presence of Si (atomic mass 28.086) in the modified MP (Fig. 1O), compared to the control cores (Fig. 1N), confirms the successful deposition of the SiO₂ layer. Additionally, the detection of Cu in both core and

modified MPs is attributed to the background material used during sample analysis.

3.2. Effect of synthesis volume variation of MPs on NA extraction

One of the crucial parameters during the synthesis of MPs is the batch volume. MPs fabricated under different synthesis volumes may exhibit variations in size, uniformity, magnetic properties, morphology, and surface characteristics. Each of these factors can play a significant role in their effectiveness in NA extraction. While a significant part of research in this field, especially the academic one, is satisfied with producing MPs in small synthesis volumes, scaling up production to larger volumes poses a considerable challenge. For MPs production to become commercially viable, it is essential to maintain critical properties and parameters when transitioning from small-scale to large-scale production. However, achieving this scalability while preserving the desired properties of MPs is highly complex and often accompanied by difficulties. We evaluated the impact of synthesis volume on extraction efficiency by comparing MPs synthesized in two different batch sizes.

We evaluated and compared the NA extraction efficiency of MPs produced in 1 L and 5 L batch sizes. DNA extraction efficiency, represented by CMV in the FAM channel, was assessed using the highest concentration of 10^4 IU \cdot mL $^{-1}$. MPs/1 L demonstrated the highest extraction efficiency with the lowest Ct value of 28.20 (Fig. 2A). For

MPs/5 L, the Ct values showed minimal deviation, with only a minor outlier of 0.71 Ct compared to MPs/1 L. At lower DNA concentrations, the MPs/5 L batch yielded higher DNA recovery, reflected in a lower Ct value of 31.65. This represents an improvement of 1.00 Ct compared to the MPs/1 L batch at the same concentration. In the HEX channel, which captures internal control, MPs/5 L exhibited the lowest difference in Ct values between positive and negative samples, ranging from 29.87 to 30.27, with a difference of only 0.40 Ct (Fig. 2B). In comparison, MPs/1 L had a wider difference, with Ct values ranging from 30.07 to 30.83 (0.76 Ct gap).

When isolating RNA, represented by HCV in the FAM channel, no statistically significant differences were observed in the Ct values between samples extracted using MPs/1 L and MPs/5 L. At a concentration of 10^4 IU \cdot mL $^{-1}$, the difference in Ct values was only 0.27 Ct, and at a lower concentration of 500 IU \cdot mL $^{-1}$, the difference was just 0.19 Ct (Fig. 2C). These differences are negligible, indicating that increasing the production volume of MPs does not affect their RNA isolation efficiency. For RNA associated with internal control, samples extracted with MPs/5 L exhibited a slightly lower Ct value, with a difference of only 0.32 Ct between positive and negative samples (Fig. 2D). Furthermore, the average Ct for MPs/5 L decreased as the concentration of positive material in the samples decreased, suggesting enhanced retention of the internal control at lower concentrations. In contrast, samples extracted with MPs/1 L showed a larger difference of 1.03 Ct between samples.

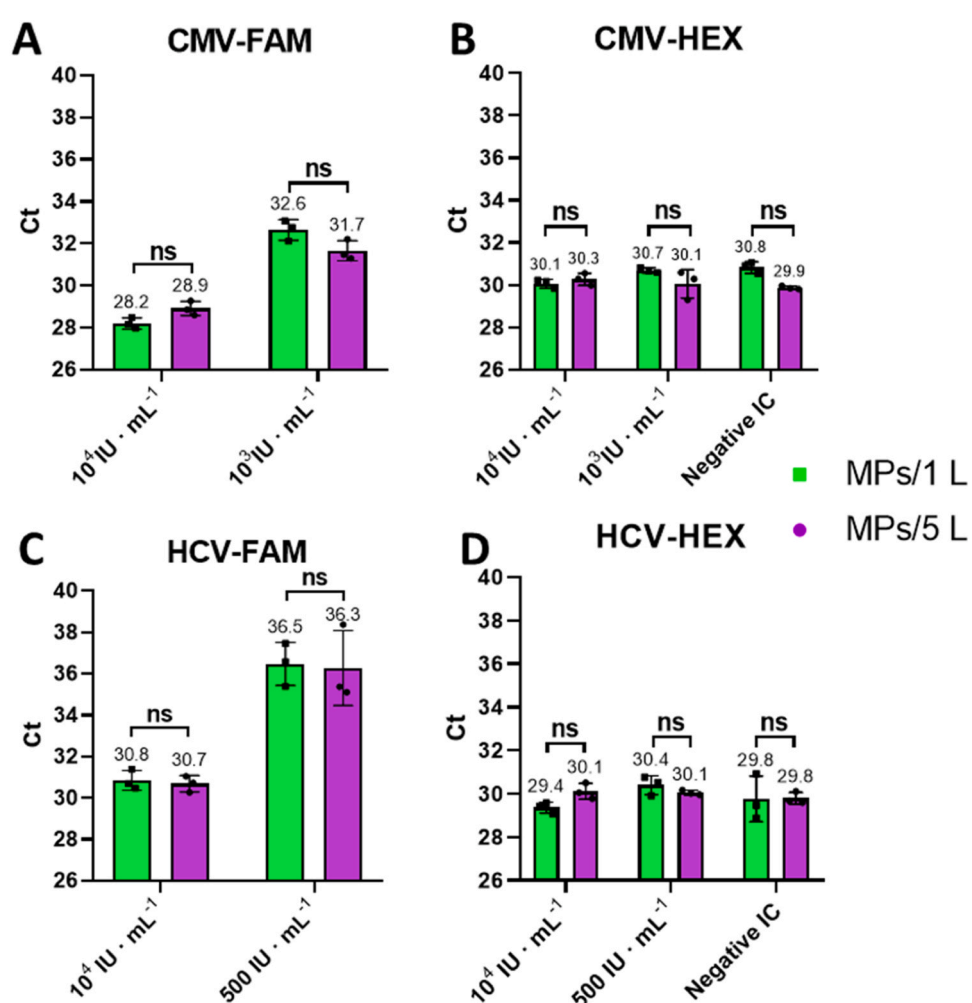


Fig. 2. (A) Ct values measured in the FAM channel for samples with varying concentrations of CMV, and (B) Ct values of the internal control detected in the HEX channel for samples containing CMV at different concentrations and CMV negative samples. (C) Ct values were recorded in the FAM channel for samples with different HCV concentrations and (D) Ct values of the internal control detected in the HEX channel for samples containing HCV at different concentrations and HCV negative samples. (ns: not significant).

While minor differences were noted, both MPs/1 L and MPs/5 L demonstrated comparable overall efficiency in RNA isolation, confirming consistent performance across batch sizes. The minor variations observed in RNA quantities are likely influenced by the presence of the internal control RNA, which may introduce competitive binding dynamics during the extraction process. When both target RNA and internal control RNA coexist within a sample, they may compete for a finite number of binding sites on the MPs, particularly under sub-saturating or limiting binding conditions [43]. This competition can result in differential extraction efficiencies between RNA species. Additionally, the secondary structure of RNA may influence binding efficiency, as regions of tightly folded RNA can hinder interaction with

the MPs' surface, thereby affecting overall recovery. The inherently low abundance of target RNA at lower concentrations further increases susceptibility to technical variability. Under such conditions, subtle inconsistencies in MPs' surface chemistry, particle batch uniformity, or buffer composition may have amplified effects on RNA recovery and downstream detection sensitivity by RT-qPCR. MPs synthesized in 1 L and 5 L batches demonstrated consistent NA extraction performance. MPs/1 L showed the highest DNA extraction efficiency at $10^4 \text{ IU} \cdot \text{mL}^{-1}$, while MPs/5 L exhibited better extraction efficiency at lower DNA concentrations and reduced the difference in internal control Ct values, reflecting better consistency. RNA extraction efficiency was comparable between batch sizes, with minimal differences in Ct values. These

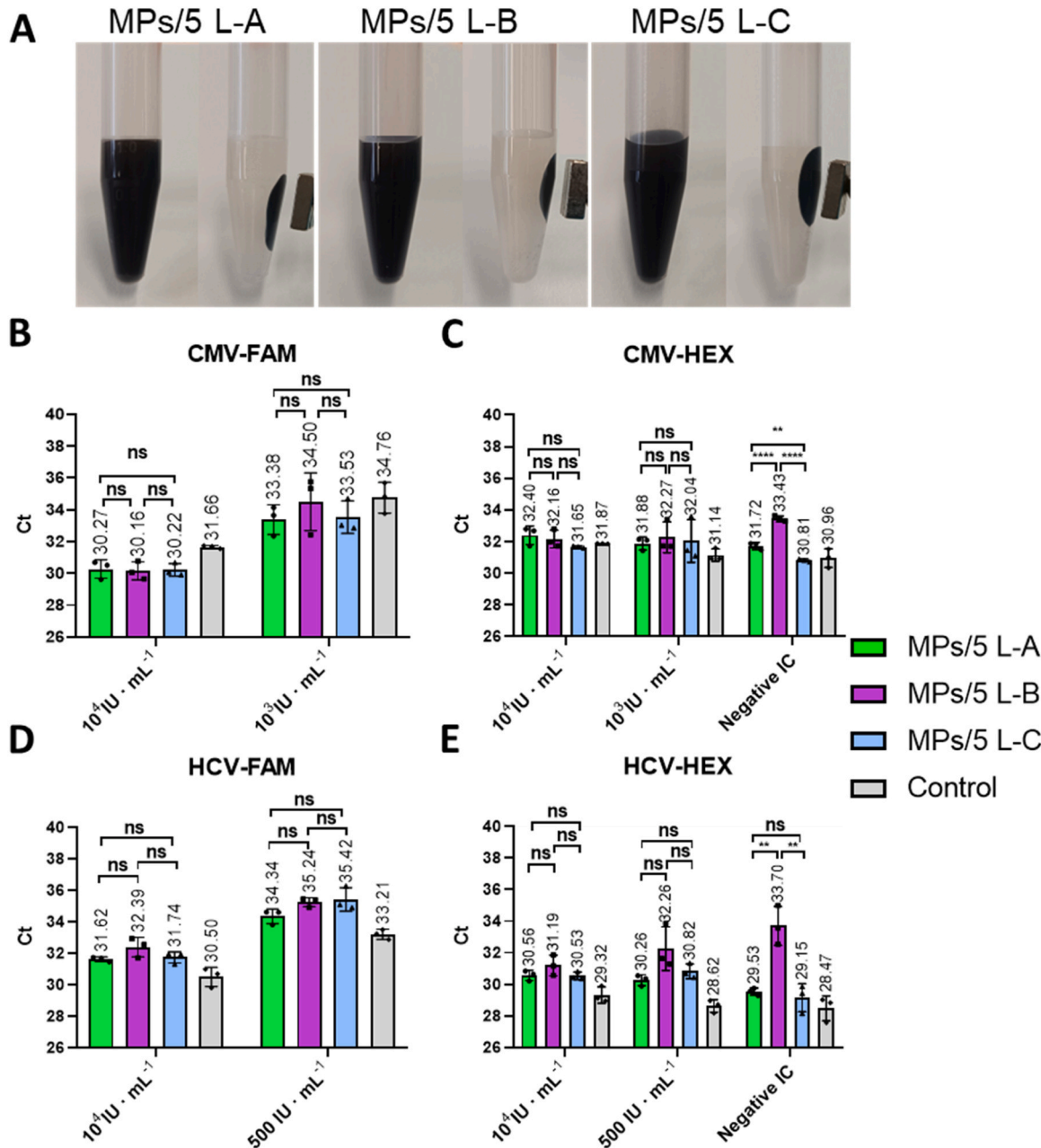


Fig. 3. (A) Photo of resuspended MPs/5 L-A, MPs/5 L-B, and MPs/5 L-C ($1 \text{ mg} \cdot \text{mL}^{-1}$) after exposition to the external magnetic field. (B) Ct values measured in the FAM channel for CMV samples at concentrations of $10^4 \text{ IU} \cdot \text{mL}^{-1}$ and $10^3 \text{ IU} \cdot \text{mL}^{-1}$. (C) Ct values for the internal control detected in the HEX channel for CMV samples at $10^4 \text{ IU} \cdot \text{mL}^{-1}$, $10^3 \text{ IU} \cdot \text{mL}^{-1}$, and CMV-negative samples. (D) Ct values were measured in the FAM channel for HCV samples at concentrations of $10^4 \text{ IU} \cdot \text{mL}^{-1}$ and $500 \text{ IU} \cdot \text{mL}^{-1}$. (E) Ct values for the internal control detected in the HEX channel for HCV samples at $10^4 \text{ IU} \cdot \text{mL}^{-1}$, $10^3 \text{ IU} \cdot \text{mL}^{-1}$, and HCV negative samples. Data are presented as the mean \pm standard deviation, derived from three independent replicates. (*: $p < 0.05$; **: $p < 0.01$; ***: $p < 0.001$; ****: $p < 0.0001$; ns: not significant).

findings confirm that scaling up to 5 L production maintains performance and enhances reliability for NA extraction.

3.3. Large-scale MPs synthesis: repeatability and extraction consistency

Increasing the scale of MPs synthesis to enable efficient NA extraction is a key goal. However, the critical challenge lies in ensuring the repeatability of MPs production, which directly impacts the consistency of nucleic acid extraction results. For MPs applications in the commercial sector, each new batch must demonstrate the same level of efficiency as previous batches, ensuring reliable performance. Several factors can compromise the efficiency of NA extraction if MPs production is not reproducible, such as variations in particle size and shape, differences in surface coverage, or the presence of undesirable by-products from the synthesis process. To evaluate the consistency and repeatability of MP synthesis and their effectiveness in NA extraction, three batches of consistently produced MPs were prepared and compared to a control.

To evaluate the repeatability and consistency of NA extraction, three batches of MPs were prepared identically in 5 L volumes and tested for their efficiency in NA isolation (Fig. 3A). Commercially available MPs from the myCROBE/croBEE 2.0 Universal Extraction Kit (GeneProof, Brno, Czech Republic) were used as controls. The Ct values for a concentration of $10^4 \text{ IU} \cdot \text{mL}^{-1}$ were nearly identical across the three tested batches, indicating excellent manufacturing and extraction consistency. Specifically, the Ct values for samples isolated using MPs/5 L-A, MPs/5 L-B, and MPs/5 L-C were 30.27, 30.16, and 30.22, respectively (Fig. 3B). Notably, the tested MPs exhibited lower average Ct values compared to the commercial MPs, indicating a potentially higher efficiency in DNA extraction at the tested CMV concentration. The difference in Ct values between the samples extracted by developed MPs and the commercial equivalent was at least 1.37 Ct in favor of the developed MPs. A lower Ct value indicates either a higher yield of viral DNA or better binding specificity between the MPs and the target DNA. In the case of a DNA concentration of $10^3 \text{ IU} \cdot \text{mL}^{-1}$, the samples extracted using the developed MPs demonstrated lower average Ct values compared to the commercial MPs, indicating higher extraction efficiency even at lower DNA concentrations. Among the developed MPs, MPs/5 L-A and MPs/5 L-C exhibited nearly identical Ct values of 33.38 and 33.53, respectively. In contrast, MPs/5 L-B showed a slightly higher Ct value of 34.50, suggesting minimal variability between batches while maintaining overall consistency.

The Ct values of the internal standard in the HEX channel varied across the three developed MPs batches, indicating inter-batch variability. Specifically, the Ct values for samples extracted using MPs/5 L-A, MPs/5 L-B, and MPs/5 L-C were 31.72, 33.43, and 30.81, respectively (Fig. 3C). Since a constant amount of UNIC was added to all samples, this variability reflects differences in extraction performance between batches. In comparison, samples obtained using commercial MPs exhibited a Ct value of 30.68, similar to MPs/5 L-C, suggesting comparable extraction efficiency for this batch. Notably, the Ct values of the internal standard for positive CMV samples in the HEX channel were influenced by the presence of CMV DNA. The internal control signals for MPs/5 L-A, MPs/5 L-B, and MPs/5 L-C were centered around a mean value of 32.00, indicating consistent isolation efficiency across batches. In contrast, the average Ct value for the commercial MPs was slightly lower at 31.50.

Compared to DNA extraction, RNA extraction using the developed MPs demonstrated significantly lower efficiency. For an RNA concentration of $10^4 \text{ IU} \cdot \text{mL}^{-1}$, the Ct values obtained from MPs/5 L-A and MPs/5 L-C were 31.62 and 31.74, respectively (Fig. 3D). These closely aligned values reflect good consistency between these batches. However, MPs/5 L-B exhibited higher Ct values, suggesting variability potentially attributable to inconsistent production. All three developed MP batches exhibited higher Ct values when extracting viral RNA represented by HCV, indicating reduced RNA extraction efficiency

compared to commercially produced MPs. This lower performance could result from a weaker binding affinity of the MP surface for RNA molecules compared to commercial MPs. Similar to the higher RNA concentration ($10^4 \text{ IU} \cdot \text{mL}^{-1}$) of HCV, the extraction efficiency at a lower RNA concentration (500 $\text{IU} \cdot \text{mL}^{-1}$) remained largely consistent. The Ct values for MPs/5 L-B and MPs/5 L-C were nearly identical, differing by only 0.01 compared to the commercial MPs. In contrast, the Ct values for samples extracted using MPs/5 L-A were more than 1.07 lower than the other two developed batches. RNA extraction results revealed significant variability between the developed MPs batches, contributing to their reduced RNA extraction efficiency relative to the commercial MPs. Notably, the commercial MPs demonstrated a greater than 0.5-log difference compared to MPs/5 L-B and MPs/5 L-C, corresponding to a Ct value difference exceeding 1.66. A difference of over 1 log, equivalent to a Ct value difference greater than 3.32, reflects a disparity of one order of magnitude in RNA yield.

For RNA extraction, represented by UNIC, samples extracted with the developed MPs showed a lower extraction efficiency of at least 1 Ct compared to those extracted with commercial MPs (Fig. 3E). The Ct values of the internal standard for positive samples were affected by the HCV extraction process. Internal control signals for MPs/5 L-A and MPs/5 L-C were centered around a mean Ct value of 30.50, whereas MPs/5 L-B showed a higher average Ct value of approximately 31.70. By comparison, the commercial MPs exhibited an average Ct value of 31.50. The variations in RNA extraction using different batches of MPs can be influenced by several factors. Variability in RNA extraction efficiency across different batches of MPs may arise from several physicochemical and procedural factors. One key contributor is inconsistency in surface functionalization. Specifically, variability in the degree or uniformity of the TEOS-based silica coating applied during MPs synthesis can influence RNA binding capacity. While DNA binding may be relatively tolerant to minor deviations in surface properties, RNA due to its single-stranded structure, greater chemical lability, and heightened sensitivity to surface charge is more susceptible to alterations in surface chemistry. Additionally, batch-specific differences in particle size distribution or aggregation behavior may also influence extraction performance. Although SEM analyses suggested overall morphological uniformity, even subtle variations in aggregation state or surface area can result in fluctuations in available binding sites and, consequently, RNA recovery efficiency. Procedural inconsistencies such as variations in the automated dispensing of MPs or extraction buffers into cartridges can further contribute to inter-batch variability. Even slight deviations can significantly affect reproducibility, particularly when handling low-input or labile RNA samples. Lastly, differences in RNA adsorption kinetics may also play a role. Variations in surface energy or zeta potential between batches can affect the thermodynamics and binding rate of RNA, especially for low abundance or single stranded species.

The developed MPs demonstrated successful large-scale synthesis of MPs with high reproducibility and efficient DNA extraction performance. The results presented higher DNA extraction efficiency than commercial MPs, with consistent Ct values throughout three tested batches and improved performance at both high and low DNA concentrations. A minimum of inter-batch variability was observed, affirming robust MPs production for DNA extraction. However, RNA extraction efficiency was lower for the developed MPs, as indicated by higher Ct values and increased variability compared to the commercial MPs. Additionally, inter-batch inconsistencies were observed in RNA extraction performance. These differences may stem from the distinct structural and chemical characteristics of RNA, its lower stability, and higher susceptibility to environmental factors during the extraction process.

3.4. MPs stability: ensuring reliability in NA isolation

The development and synthesis of MPs can be both costly and time-consuming. A crucial factor for their successful application in industrial and clinical settings is their stability, which impacts not only their

chemical and physical properties but also their potential for reuse. Stable MPs that can be stored and reused significantly lower the overall costs for laboratories and diagnostic facilities. The stability of MPs is influenced by several factors, including their size, morphology, the chemical composition of the magnetic core, the type of surface modification, and storage conditions. Developing stable MPs requires meticulous optimization of their fabrication process, a well-thought-out structural design, and thorough characterization of their properties. Ensuring the stability of MPs is essential for achieving long-term reliability and reproducibility in NA extraction.

The stability and functionality of the two batches of MPs were evaluated over two years of storage in aqueous solutions. One month before testing, MPs were introduced into the binding buffer. At a higher CMV concentration of 10^4 IU \cdot mL $^{-1}$, the efficiency of CMV extraction detected in the FAM channel demonstrated excellent stability in both MPs batches. The average Ct values for FAM signal detection were 27.38 for batch MPs/5 L-A and 27.72 for batch MPs/5 L-B (Fig. 4A). Compared to the control MPs, which exhibited an average Ct value of 27.94, the developed MPs demonstrated higher extraction efficiency even after one year of storage. At the lower CMV concentration of 10^3 IU \cdot mL $^{-1}$, the differences between the two developed batches were negligible, with average Ct values of 31.00 for batch MPs/5 L-A and 31.03 for batch MPs/5 L-B. The minimal difference of only 0.03 Ct indicates excellent synthesis homogeneity between the batches. Compared to the control MPs, which had an average Ct value of 31.67, the observed difference of 0.64 Ct indicates that the developed MPs exhibited higher extraction efficiency even at lower CMV concentrations.

The extraction efficiency of plasmid DNA, used as an internal control

in positive samples (10^4 IU \cdot mL $^{-1}$, 10^3 IU \cdot mL $^{-1}$) and detected in the HEX channel, showed some differences between the developed MPs batches and the control MPs. For Batch MPs/5 L-A, the average Ct values were 32.50 for a concentration of 10^4 IU \cdot mL $^{-1}$ and 33.03 for 10^3 IU \cdot mL $^{-1}$. In contrast, Batch MPs/5 L-B exhibited average Ct values of 33.79 for 10^4 IU \cdot mL $^{-1}$ and 32.96 for 10^3 IU \cdot mL $^{-1}$ (Fig. 4B). The median Ct value across all these results was approximately 33, with the largest observed difference being 0.79 Ct. This variation could be attributed to competition between viral CMV particles and plasmid DNA during both the extraction and PCR processes, where CMV DNA is likely prioritized. In comparison, the control MPs showed average Ct values of 31.94 for 10^4 IU \cdot mL $^{-1}$ and 31.92 for 10^3 IU \cdot mL $^{-1}$. The difference between the developed MPs and the control MPs was approximately 1 Ct, potentially due to the significantly higher amount of extracted viral DNA using the synthesized MPs, which may have influenced plasmid DNA amplification efficiency. For negative samples in the HEX channel, the differences between developed MPs and control MPs were minimal. The average Ct value for Batch MPs/5 L-A was 32.17, identical to the control MPs (32.17 Ct), while Batch MPs/5 L-B exhibited a slightly higher value of 32.76 Ct, with a difference of 0.59 Ct. This suggests that Batch MPs/5 L-B may have slightly lower plasmid DNA extraction efficiency compared to Batch MPs/5 L-A, as indicated by the higher Ct values for plasmid DNA.

The extraction of HCV, detected via the FAM channel at a higher concentration of 10^4 IU \cdot mL $^{-1}$, demonstrated slightly better extraction efficiency and stability for the control MPs. The average Ct value for this RNA concentration was 29.35 for batch MPs/5 L-A and 30.40 for batch MPs/5 L-B (Fig. 4C). In comparison, the control MPs exhibited an

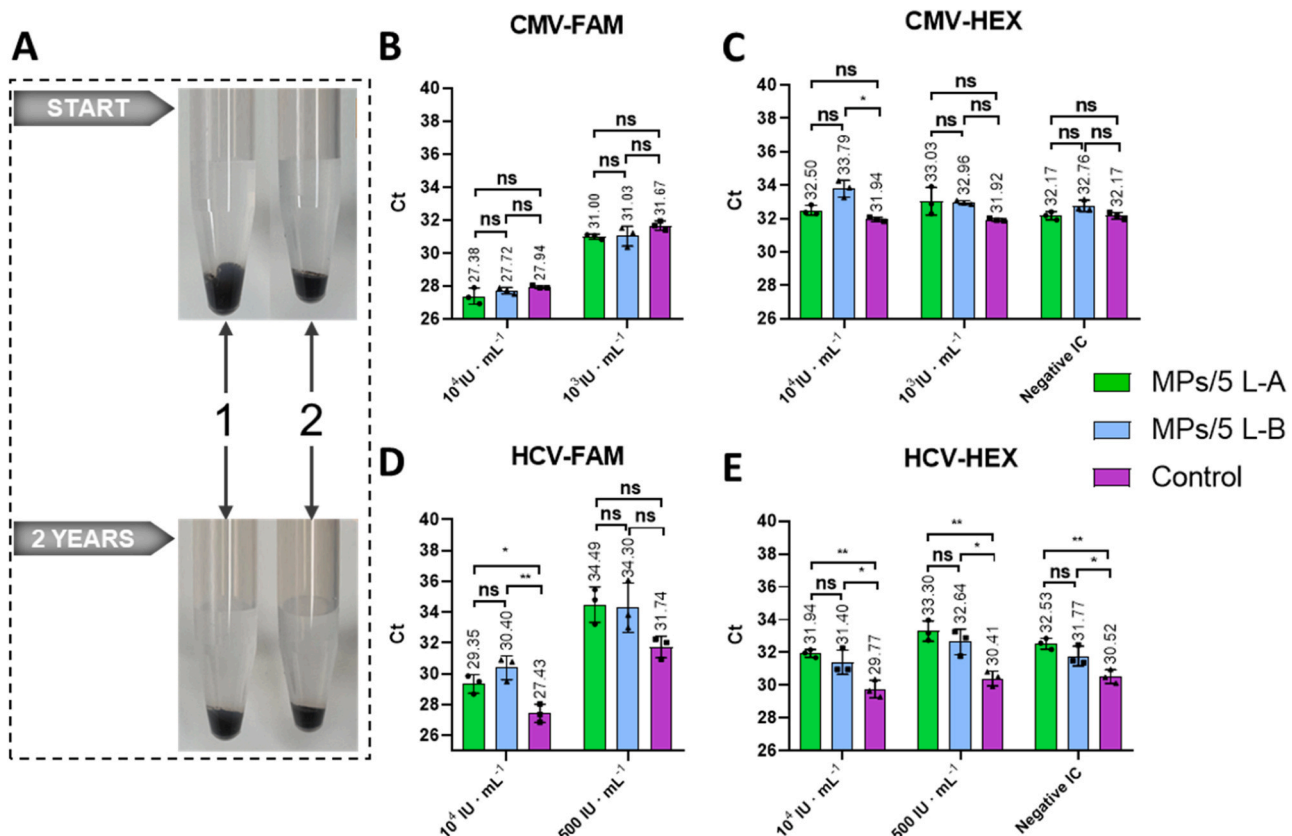


Fig. 4. (A) Representative images of MPs immediately after synthesis and after two years of storage, demonstrating their stability. 1: MPs/5 L-A; 2: MPs/5 L-B. (B) RT-qPCR results confirm the stability of MPs and the extraction efficiency of CMV, as indicated by fluorescence signals in the FAM channel at two concentrations: 10^4 IU \cdot mL $^{-1}$ and 10^3 IU \cdot mL $^{-1}$. Additionally, Ct values for the internal control, detected in the HEX channel (C), are presented for samples containing CMV at a concentration of 10^4 IU \cdot mL $^{-1}$, 10^3 IU \cdot mL $^{-1}$, and CMV negative samples. Results showing the stability of MPs and the extraction efficiency of HCV in FAM channel (D) at two concentrations: 10^4 IU \cdot mL $^{-1}$ and 500 IU \cdot mL $^{-1}$ and Ct values of the internal control detected in the HEX channel (E) for samples containing CMV at concentration 10^4 IU \cdot mL $^{-1}$, 500 IU \cdot mL $^{-1}$ and HCV negative samples (*: $p < 0.05$, **: $p < 0.01$; ns: not significant).

average Ct value of 27.43. These differences are statistically significant in favor of the control MPs. At a lower RNA concentration, no significant differences were observed between the developed and control MPs, with average Ct values of 34.49 for Batch MPs/5 L-A, 34.30 for Batch MPs/5 L-B, and 31.74 for control MPs.

The extraction of viral RNA from internal control in positive samples, detected in the HEX channel, revealed no significant differences between the developed MPs but significant differences compared to the control MPs. For batch MPs/5 L-A, the average Ct values were 31.94 at a higher concentration (10^4 IU \cdot mL $^{-1}$) and 33.30 at a lower concentration (500 IU \cdot mL $^{-1}$). Similarly, for batch MPs/5 L-B, the average Ct values were 31.40 for 10^4 IU \cdot mL $^{-1}$ and 32.64 for 500 IU \cdot mL $^{-1}$ (Fig. 4D), indicating minimal variation and comparable RNA extraction efficiency between the synthesized MPs batches. In contrast, the control MPs exhibited lower average Ct values of 29.77 for 10^4 IU \cdot mL $^{-1}$ and 30.41 for 500 IU \cdot mL $^{-1}$. The differences between the developed and control MPs ranged from 1.63 to 2.89 Ct, indicating statistically significant variations in extraction efficiency. For negative samples detected in the HEX channel, the average Ct value for batch MPs/5 L-A was 32.53, while for batch MPs/5 L-B, it was 31.77, with a difference of only 0.76 Ct. This difference is not statistically significant, indicating that both developed MPs batches exhibit comparable RNA extraction efficiency. In comparison, the control MPs had a lower average Ct value of 30.52. The differences between Batch MPs/5 L-A and the control MPs (2.01 Ct) and between Batch MPs/5 L-B and the control MPs (1.25 Ct) suggest that the control MPs demonstrated higher efficiency in extracting viral RNA, both from the HCV pathogen and the internal control. The decline in RNA extraction efficiency observed after two years of MPs storage may result from physicochemical alterations at the particle surface. One plausible mechanism is the hydrolytic degradation, leaching, or reorganization of surface silanol groups on the TEOS-based silica coating, particularly under prolonged aqueous storage conditions [44,45]. These processes can reduce the density, distribution, or accessibility of functional groups critical for RNA adsorption. Surface fouling may also contribute to reduced performance. Despite controlled storage conditions, prolonged exposure to storage buffers may lead to the accumulation of trace contaminants, such as organic residues or ionic species, which can adsorb to the particle surface and interfere sterically or electrostatically with RNA binding [44]. In addition, changes in surface charge characteristics over time may affect electrostatic interactions essential for RNA capture. The isoelectric point of silica-based MPs (pH \sim 3.3) implies that they carry a strong negative charge at neutral pH. Over time, changes in surface charge due to hydrolysis or adsorption could alter electrostatic interactions with RNA, particularly in chaotic environments. To mitigate these effects, surface modification strategies could be employed to enhance long-term stability and RNA specificity. For example, functionalization with amine groups may increase binding affinity through electrostatic attraction to the RNA phosphate backbone. Alternatively, the application of protective polymer coatings or the incorporation of stabilizing agents could help preserve the structural and chemical integrity of the MPs during extended storage, thereby maintaining their extraction efficiency [46].

The developed MPs demonstrated significant stability and extraction efficiency over a one-year storage period. For DNA extraction, both MPs batches outperformed the control MPs, yielding lower Ct values and confirming their enhanced efficiency. However, for HCV RNA extraction, the control MPs outperformed the synthesized MPs, particularly at higher RNA concentrations, where statistically significant differences were observed. The reduced RNA extraction efficiency of the developed MPs compared to the control is not related to their stability, as the same trend has been observed in other experiments. Despite this, RNA extraction efficiency between the two synthesized batches remained consistent, demonstrating batch-to-batch reproducibility.

3.5. Impact of lyophilized and hydrated MPs forms on NA isolation efficiency

Lyophilization (freeze-drying) is an alternative method for water removal compared to conventional heat-based techniques. It involves freezing the sample followed by pressure reduction to facilitate the sublimation of ice. Lyophilization is widely used in the pharmaceutical and food industries, as heating can degrade labile molecules, particularly biomacromolecules. Another advantage of lyophilized MPs is their potential integration into lyophilized reaction mixtures designed for subsequent analyses. These mixtures are intended for testing outside the laboratory and should withstand various environmental conditions. However, despite its advantages, lyophilization exposes particles to various stressors during dehydration, including changes in pH, ionic strength, and mechanical stress caused by ice formation. Nonetheless, lyophilization can enhance the shelf life of MPs, as discussed in the previous chapter. Lyophilized MPs require rehydration in water or an isolation buffer before use. In contrast, hydrated MPs are instantly ready for use, but they tend to be more susceptible to degradation during storage. Understanding these differences and selecting the appropriate type of MPs is essential for ensuring efficient NA extraction and producing reliable results.

One of the critical factors influencing the extraction efficiency of MPs is their physical state – whether they are lyophilized into a dry powder or hydrated in a water suspension. Dehydration of MPs during lyophilization can influence their subsequent dispersibility, surface properties, and binding capacity [47]. Fig. 5A shows a photo of lyophilized MPs and MPs after rehydration. Below, there are corresponding SEM micrographs of MPs, which do not show any apparent differences. The extraction efficiency was evaluated for two batches of MPs in both hydrated and lyophilized forms (Fig. 5B). The results indicate that hydrated MPs exhibit significantly higher DNA extraction efficiency compared to their lyophilized analogs.

In the case of DNA extraction of the virus represented by CMV and detected in the FAM channel, the higher concentration of 10^4 IU \cdot mL $^{-1}$ showed significant differences between hydrated and lyophilized MPs (Fig. 5C). In both batches, the mean Ct values obtained for the hydrated MPs at this concentration were 30.27 for batch MPs/5 L-A and 30.22 for batch MPs/5 L-B. In contrast, the lyophilized MPs showed an average Ct value of 32.61 for batch MPs/5 L-A, reflecting a difference of 2.34 Ct. This corresponds to a greater than 0.5 log reduction (1.66 Ct), which is statistically significant. An even larger difference was observed for batch MPs/5 L-B, where the lyophilized MPs showed an average Ct value of 33.72. The difference of 3.5 Ct between hydrated and lyophilized MPs for this batch indicates more than 1 log reduction (3.32 Ct), suggesting that hydrated MPs achieve at least 10-fold greater extraction efficiency than the lyophilized form. At a lower concentration of 10^3 IU \cdot mL $^{-1}$ for CMV detected in the FAM channel, the differences between hydrated and lyophilized MPs are less significant due to the reduced amount of DNA used. Nevertheless, the differences remain statistically significant. For batch MPs/5 L-A, the average Ct value for hydrated MPs was 33.38, compared to 35.08 for lyophilized MPs, resulting in a difference of 1.70 Ct, which is equivalent to a 0.5-log reduction (Fig. 5C). A larger difference was observed for MPs/5 L-B, where hydrated MPs presented a Ct value of 33.53. In contrast, the lyophilized MPs exhibited a Ct value of 35.84. This difference of 2.31 Ct is more than 0.5 log, further highlighting the hydrated MPs' higher extraction efficiency.

The extraction of plasmid DNA from positive samples detected in the HEX channel demonstrated consistent patterns across batches. For batch MPs/5 L-A, the average Ct values for hydrated MPs were 32.40 for samples with a higher concentration (10^4 IU \cdot mL $^{-1}$) and 31.88 for samples with a lower concentration (10^3 IU \cdot mL $^{-1}$) (Fig. 5DE). In comparison, the lyophilized MPs provided Ct values of 34.02 and 33.33 for the higher and lower DNA concentrations, respectively. The differences between hydrated and lyophilized MPs were 1.58 Ct for the high positive samples (10^4 IU \cdot mL $^{-1}$) and 1.45 Ct for the low positive samples

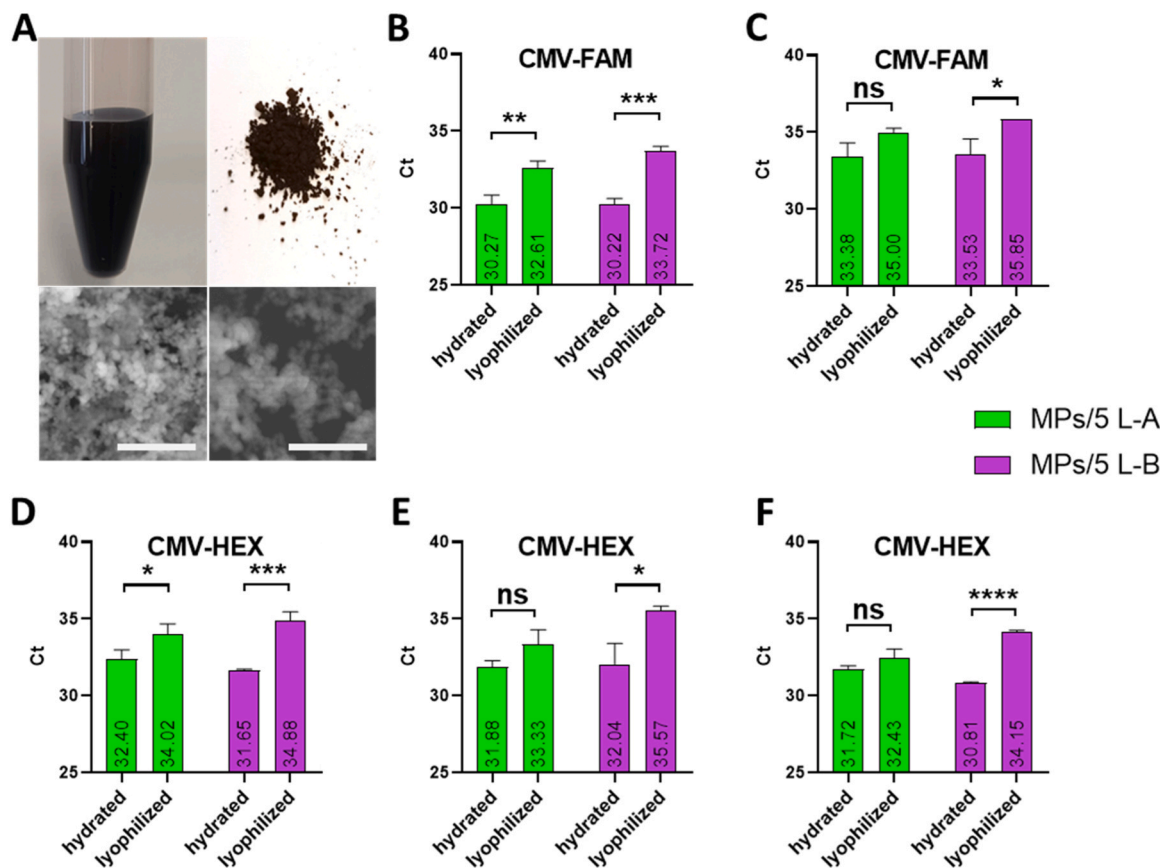


Fig. 5. RT-qPCR results showing the effect of lyophilized and hydrated MPs on the extraction efficiency of CMV. (A) Present of the MPs in a water solution with the content of $1 \text{ mg} \cdot \text{mL}^{-1}$, including an SEM micrograph. Additionally, 1 mg of lyophilized MPs is shown alongside an SEM micrograph of the lyophilized MPs after rehydration in an aqueous solution (scale bar: 500 nm). (B) and (C) present the Ct values detected in the FAM channel for CMV at concentrations of $10^4 \text{ IU} \cdot \text{mL}^{-1}$ and $10^3 \text{ IU} \cdot \text{mL}^{-1}$. (D) Shows the Ct values in the HEX channel for samples containing CMV at $10^4 \text{ IU} \cdot \text{mL}^{-1}$, (E) for CMV at $10^3 \text{ IU} \cdot \text{mL}^{-1}$, and (F) for CMV negative samples. Data are presented as the mean \pm standard deviation, derived from three independent replicates. (*: $p < 0.05$; **: $p < 0.01$; ***: $p < 0.001$; ****: $p < 0.0001$; ns: not significant).

($10^3 \text{ IU} \cdot \text{mL}^{-1}$). These comparable differences suggest that hydrated MPs consistently exhibit better plasmid DNA binding efficiency than lyophilized MPs. A similar trend was observed for negative samples detected in the HEX channel, although the difference between hydrated and lyophilized MPs was lower. Hydrated MPs provided an average Ct value of 31.72, compared to 32.43 for lyophilized MPs, representing a difference of 0.71 Ct (Fig. 5F). It should be noted that negative samples did not contain plasmid DNA, which may have influenced the differences observed in the extraction efficiency in the HEX channel. Batch MPs/5 L-B demonstrated consistent extraction of plasmid DNA from both positive and negative samples, with similar patterns observed across all replicates. Notably, hydrated MPs presented more than 1 log higher DNA extraction efficiency than lyophilized MPs across two sample types. For low positive CMV samples, hydrated MPs achieved an average Ct value of 32.04 in the HEX channel, significantly lower than the 35.57 Ct obtained with lyophilized MPs, indicating higher sensitivity. Negative samples also showed improved performance with hydrated MPs, yielding an average Ct value of 30.81 compared to 34.15 for lyophilized MPs. For highly positive samples, the difference between the hydrated and lyophilized MPs was lower but still appreciable. Hydrated MPs resulted in an average Ct value of 31.65 compared to 34.88 for lyophilized MPs, reflecting an average difference of 3.23 Ct. This difference is approximately equivalent to 1 log, further underscoring the higher efficiency of hydrated MPs for plasmid DNA extraction.

In summary, hydrated MPs consistently outperformed lyophilized MPs, showing significantly lower Ct values across high ($10^4 \text{ IU} \cdot \text{mL}^{-1}$) and low ($10^3 \text{ IU} \cdot \text{mL}^{-1}$) DNA concentrations in both the FAM and HEX

channels. Differences ranged from 1.45 to 3.5 Ct, corresponding to up to a 1-log (10-fold) improvement in DNA extraction efficiency. For low-positive CMV samples, hydrated MPs demonstrated greater sensitivity with Ct values averaging 32.04 compared to 35.57 for lyophilized MPs. Even in negative samples, hydrated MPs achieved lower Ct values, underscoring their superior efficiency and consistency across varying DNA concentrations. The higher DNA extraction efficiency of hydrated MPs compared to lyophilized MPs can be attributed to the preservation of surface functionality and binding efficiency in the hydrated form. The lyophilization process can potentially modify the physical structures, surface charge, or binding sites of MPs, resulting in reduced interactions with NA. Hydrated MPs likely maintain optimal dispersion and active surface area when incorporated into isolation buffers, thereby enhancing their ability to bind NA efficiently. This is facilitated by the presence of chaotropic salts in the binding buffer, which promotes the formation of a salt bridge between the negatively charged MPs and NA. In contrast, lyophilized MPs may not fully rehydrate upon introduction into the binding buffer or may aggregate, reducing their effective binding surface and, consequently, their NA extraction efficiency. Despite being added to the binding buffer a week before extraction, it is unlikely that the lyophilized MPs achieved complete rehydration, further compromising their efficiency. The physical form of MPs significantly influences their extraction properties, including NA binding capacity, separation kinetics, and the purity and quality of the extracted molecules. Lyophilization can alter the structure of surface modifications, potentially affecting binding affinity or increasing non-specific adsorption. In contrast, properly stored hydrated MPs provide

more stable and consistent binding conditions, ensuring reliable performance in nucleic acid extraction. To maintain the functionality and extraction efficiency of lyophilized MPs, several strategies may be considered. Incorporating lyoprotectants such as trehalose, mannitol, or polyethylene glycol during the lyophilization process can help preserve the structural integrity and surface chemistry of the MPs by minimizing ice crystal formation and preventing surface collapse [48]. Another potential approach is to package the lyophilized MPs in vacuum-sealed or inert gas-filled containers, which can limit oxidation and moisture-driven degradation during storage [49]. Additionally, using alternative surface modifications that are more compatible with lyophilization could enhance the long-term stability and performance of MPs. However, these improvements introduce added complexity and cost to the manufacturing process. As a result, they may not align with the practical requirements and cost-efficiency preferences of large-scale MPs producers.

The influence of hydrated and lyophilized MPs on the extraction of pathogenic RNA, represented by HCV, was evaluated. RNA extraction was assessed using the FAM detection channel for two HCV concentrations: $10^4 \text{ IU} \cdot \text{mL}^{-1}$ and $500 \text{ IU} \cdot \text{mL}^{-1}$. Similar to the results observed for DNA extraction of CMV, hydrated MPs demonstrated higher efficiency in extracting RNA molecules compared to lyophilized MPs. However, the observed differences in RNA extraction efficiency were less pronounced ($< 0.5 \log$) than those observed for DNA extraction.

The results for MPs/5 L-A demonstrated that HCV RNA extraction using hydrated MPs at a concentration of $10^4 \text{ IU} \cdot \text{mL}^{-1}$ yielded an average Ct value of 31.62, while lyophilized MPs produced an average Ct value of 32.14 (Fig. 6A). The difference of 0.52 Ct is not statistically

significant. However, a higher difference of 1.24 Ct was observed for this batch at HCV concentration of $500 \text{ IU} \cdot \text{mL}^{-1}$, where hydrated MPs showed an average Ct value of 34.34, compared to 35.48 for lyophilized MPs (Fig. 6B). This indicates that the difference between hydrated and lyophilized MPs is more significant at lower HCV concentrations. For MPs/5 L-B, the differences between hydrated and lyophilized MPs were minimal and consistent across both HCV concentrations. At $10^4 \text{ IU} \cdot \text{mL}^{-1}$, the Ct values differed by only 0.29, while at $500 \text{ IU} \cdot \text{mL}^{-1}$, the difference was 0.57. The extraction of RNA molecules from the internal control demonstrated a pattern similar to the extraction of HCV RNA. Samples extracted by hydrated MPs/5 L-A showed higher efficiency in the isolation of internal control RNA from both positive and negative samples. For samples with a concentration of $10^4 \text{ IU} \cdot \text{mL}^{-1}$, the average Ct value for internal control RNA extracted using hydrated MPs was 30.56, compared to 30.83 for lyophilized MPs, indicating a difference of 0.27 Ct (Fig. 6C). For samples with a concentration of $500 \text{ IU} \cdot \text{mL}^{-1}$, the average Ct value for hydrated MPs was 30.26, while for lyophilized MPs, it was 31.20, resulting in a slightly higher difference of 0.94 Ct (Fig. 6D). The lower Ct values observed for both hydrated and lyophilized MPs in low-concentration positive samples ($500 \text{ IU} \cdot \text{mL}^{-1}$) can be attributed to reduced competition between internal control RNA and HCV RNA molecules during RT-PCR analysis. For negative samples, where no HCV RNA is present, the Ct values were even lower. Specifically, hydrated MPs yielded an average Ct value of 29.53, compared to 30.16 for lyophilized MPs, resulting in a difference of 0.63 Ct (Fig. 6E). Hydrated MPs/5 L-B demonstrated higher efficiency in extracting internal control RNA from positive samples. For samples with a concentration of $10^4 \text{ IU} \cdot \text{mL}^{-1}$, the average Ct value for internal control RNA extracted using

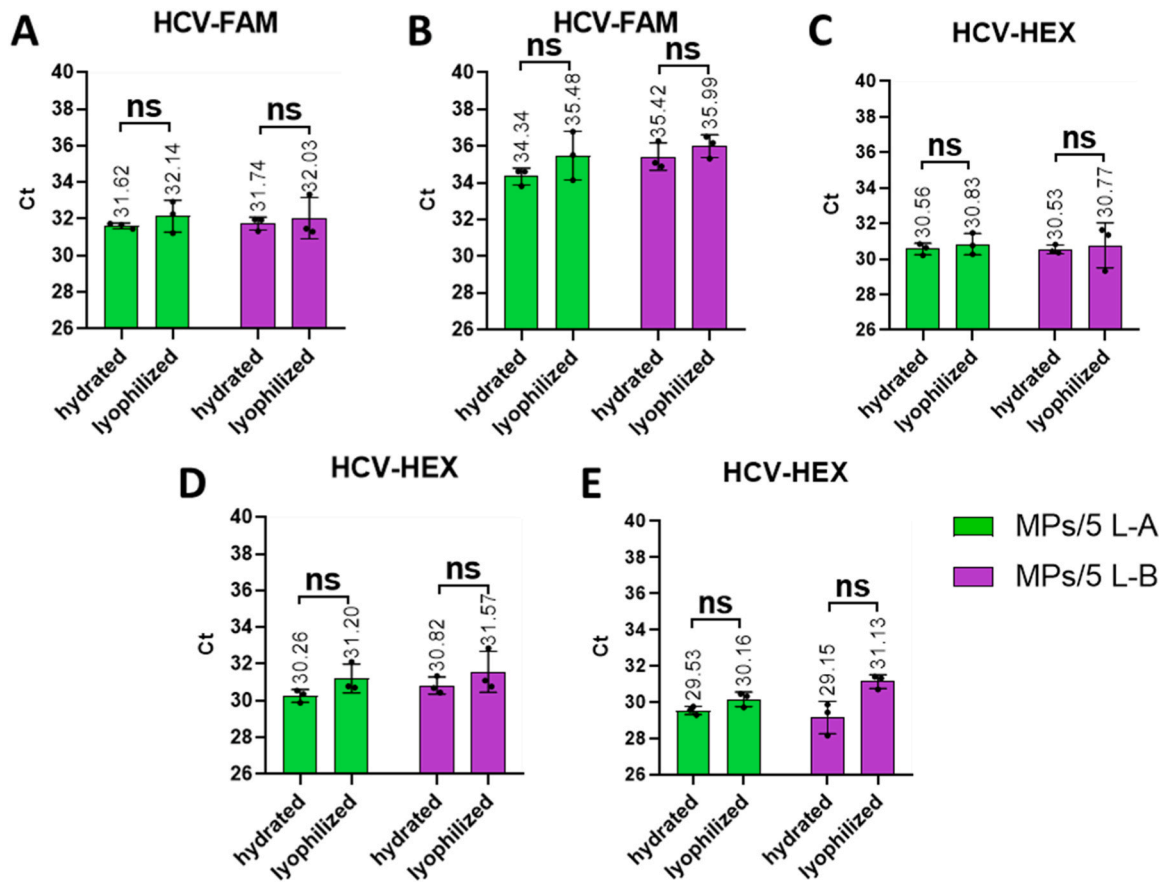


Fig. 6. RT-qPCR analysis assessing the impact of lyophilized and hydrated MPs on HCV extraction efficiency. Diagrams (A) and (B) present Ct values measured in the FAM channel for HCV at concentrations of $10^4 \text{ IU} \cdot \text{mL}^{-1}$ and $500 \text{ IU} \cdot \text{mL}^{-1}$. Graphs (C), (D), and (E) show the Ct values obtained in the HEX channel for internal controls in samples with HCV at $10^4 \text{ IU} \cdot \text{mL}^{-1}$, $500 \text{ IU} \cdot \text{mL}^{-1}$, and without HCV, respectively. Data are presented as the mean \pm standard deviation, calculated from triplicate measurements. (ns: not significant).

hydrated MPs was 30.53, compared to 30.77 for lyophilized MPs, indicating a difference of 0.24 Ct. For samples with a concentration of 500 IU · mL⁻¹, the average Ct value for hydrated MPs was 30.82, whereas for lyophilized MPs, it was 31.57, showing a slightly higher difference of 0.75 Ct. A similar pattern was observed in RNA internal control extraction from negative samples. Hydrated MPs yielded an average Ct value of 29.15, while lyophilized MPs had a higher Ct value of 31.13, indicating better RNA extraction efficiency for hydrated MPs.

The results indicate that hydrated MPs generally outperform lyophilized MPs in RNA extraction efficiency, particularly at lower concentrations of HCV RNA (500 IU · mL⁻¹). This trend is consistent across positive samples, where hydrated MPs yield lower Ct values, suggesting more efficient RNA recovery. However, the differences are less pronounced at higher HCV concentrations (10⁴ IU · mL⁻¹), where both hydrated and lyophilized MPs perform similarly. This could imply that the extraction method plays a more critical role when RNA is present in lower quantities. For negative samples, the unexpectedly higher efficiency of lyophilized MPs in internal control RNA extraction, along with increased variability, suggests that the functional surface area of both hydrated and lyophilized MPs may be more specifically optimized for double-stranded DNA binding under the binding conditions of the kit used.

4. Conclusion

This study demonstrates the successful synthesis, characterization, and application of TEOS modified MPs for automated NA extraction. By scaling up the synthesis process from 1 L to 5 L, we achieved reproducible MPs with consistent physicochemical properties and extraction performance. Our findings confirm that MPs synthesized in larger volumes maintain their efficiency, showing minimal batch-to-batch variability in DNA extraction. While RNA recovery exhibited slightly higher variability, the developed MPs performed comparably to or better than commercial alternatives in DNA isolation. Furthermore, we investigated the impact of MPs' physical state on extraction efficiency. Hydrated MPs consistently outperformed their lyophilized counterparts, highlighting the importance of storage conditions in maintaining surface functionality and extraction efficiency. Long-term stability testing over a two-year period confirmed that MPs maintain their extraction performance, reinforcing their suitability for clinical and research applications. The developed MPs exhibit potential for integration into clinical molecular diagnostic platforms, particularly in high-throughput infectious disease screening, automated laboratory systems, and point-of-care microfluidic devices. Their scalability, high extraction efficiency, and long-term stability make them ideal for commercial nucleic acid extraction kits and decentralized diagnostic tools, including those deployed in resource-limited settings. Beyond diagnostics, these MPs have potential applications in environmental monitoring, such as pathogen detection in water samples, as well as in food safety testing and single-cell analysis. Despite these promising results, optimizing RNA extraction efficiency remains an area for improvement. Modifying the MPs' surface chemistry to introduce functional groups better suited for RNA binding could enhance RNA recovery and improve overall extraction performance.

CRediT authorship contribution statement

Pavel Švec: Investigation. **Jiří Kudr:** Writing – original draft, Conceptualization. **Eva Jansová:** Writing – review & editing. **Milos Dendis:** Writing – review & editing. **Ondrej Zitka:** Writing – review & editing, Funding acquisition. **Martin Ženka:** Writing – original draft, Validation, Conceptualization. **Zbyněk Šplíchal:** Writing – review & editing, Writing – original draft, Formal analysis. **Petra Stejskalová:** Writing – original draft, Validation, Project administration, Investigation, Conceptualization.

Declaration of Competing Interest

The authors declare that they have no known competing financial interests or personal relationships that could have appeared to influence the work reported in this paper.

Acknowledgements

We acknowledge the financial support of Grant No. TN02000017 from the Technology Agency of the Czech Republic (National Centre for Biotechnology in Veterinary Medicine), and the ERDF “Multidisciplinary research to increase application potential of nanomaterials in agricultural practice” No. CZ.02.1.01/0.0/0.0/16_025/0007314.

Data availability

Data will be made available on request.

References

- [1] X.M. Pei, M.H.Y. Yeung, A.N.N. Wong, H.F. Tsang, A.C.S. Yu, A.K.Y. Yim, S.C. Wong, Targeted sequencing approach and its clinical applications for the molecular diagnosis of human diseases, *Cells* 12 (2023).
- [2] A. Sun, P. Vopářilová, X. Liu, B. Kou, T. Řezníček, T. Lednický, S. Ni, J. Kudr, O. Zitka, Z. Fohlerová, P. Pajer, H. Zhang, P. Neužil, An integrated microfluidic platform for nucleic acid testing, *Microsynt. Nanoeng.* 10 (2024) 66.
- [3] S.C. Tan, B.C. Yiap, DNA, RNA, and protein extraction: the past and the present, *J. Biomed. Biotechnol.* 2009 (2009) 574398.
- [4] S. Zhang, X. Li, J. Wu, L. Coin, J. O'Brien, F. Hai, G. Jiang, Molecular methods for pathogenic bacteria detection and recent advances in wastewater analysis, *Water* (2021).
- [5] Q. Liu, X. Jin, J. Cheng, H. Zhou, Y. Zhang, Y. Dai, Advances in the application of molecular diagnostic techniques for the detection of infectious disease pathogens (Review), *Mol. Med. Rep.* 27 (2023).
- [6] H. Satam, K. Joshi, U. Mangrolia, S. Waghoor, G. Zaidi, S. Rawool, R.P. Thakare, S. Banday, A.K. Mishra, G. Das, S.K. Malonia, Next-generation sequencing technology: current trends and advancements, *Biology* 12 (2023).
- [7] G.W. Procop, Molecular diagnostics for the detection and characterization of microbial pathogens, *Clin. Infect. Dis.* 45 (2007) S99–S111.
- [8] M.N. Emaus, M. Varona, D.R. Eitzmann, S.-A. Hsieh, V.R. Zeger, J.L. Anderson, Nucleic acid extraction: fundamentals of sample preparation methodologies, current advancements, and future endeavors, *TrAC Trends Anal. Chem.* 130 (2020) 115985.
- [9] P. Li, M. Li, D. Yue, H. Chen, Solid-phase extraction methods for nucleic acid separation. A review, *J. Sep. Sci.* 45 (2021) 172–184.
- [10] N. Ali, R.C.P. Rampazzo, A.D.T. Costa, M.A. Krieger, Current nucleic acid extraction methods and their implications to point-of-care diagnostics, *Biomed. Res. Int.* 2017 (2017) 9306564.
- [11] R. Barnett, G. LarsonA Phenol-Chloroform Protocol for Extracting DNA from Ancient Samples, in: B. Shapiro, M. Hofreiter (Eds.) ANCIENT DNA: METHODS AND PROTOCOLS, 2012, pp. 13–19..
- [12] J.F. Regan, M.R. Furtado, M.G. Brevnov, J.A. Jordan, A sample extraction method for faster, more sensitive PCR-based detection of pathogens in blood culture, *J. Mol. Diagn.* 14 (2012) 120–129.
- [13] É. Carthy, B. Hughes, E. Higgins, P. Early, C. Merne, D. Walsh, A. Parle-McDermott, D.J. Kinahan, Automated solid phase DNA extraction on a lab-on-a-disc with two-degrees of freedom instrumentation, *Anal. Chim. Acta* 1280 (2023) 341859.
- [14] R.M. McCormick, A solid-phase extraction procedure for DNA purification, *Anal. Biochem.* 181 (1989) 66–74.
- [15] A. Ayoib, U. Hashim, S.C.B. Gopinath, M.K. Md Arshad, DNA extraction on biochip: history and preeminence over conventional and solid-phase extraction methods, *Appl. Microbiol. Biotechnol.* 101 (2017) 8077–8088.
- [16] T. Dang, S. Bodaghi, F. Osman, J. Wang, T. Rucker, S.-H. Tan, A. Huang, D. Pagliaccia, S. Comstock, I. Lavagi-Craddock, K.R. Gadhave, P. Quijia-Lamina, A. Mitra, B. Ramirez, G. Uribe, A. Syed, S. Hammado, I. Mimou, R. Campos, S. Abdulnour, M. Voeltz, J. Bae, E. Dang, B. Nguyen, X. Chen, N. Siddiqui, Y. T. Hsieh, S. Abu-Hajar, J. Kress, K. Weber, G. Vidalakis, A comparative analysis of RNA isolation methods optimized for high-throughput detection of viral pathogens in California's regulatory and disease management program for citrus propagative materials, *Front. Agron.* 4 (2022).
- [17] M.O. Hammad, Simplified protocol modification of TRIzol method for extraction of high-quality RNA yield from RNase-rich rat pancreas, *Process Biochem.* 130 (2023) 464–471.
- [18] P. Chomczynski, N. Sacchi, The single-step method of RNA isolation by acid guanidinium thiocyanate-phenol-chloroform extraction: twenty-something years on, *Nat. Protoc.* 1 (2006) 581–585.
- [19] L.S. Toni, A.M. Garcia, D.A. Jeffrey, X. Jiang, B.L. Stauffer, S.D. Miyamoto, C.C. Sucharov, Optimization of phenol-chloroform RNA extraction, *MethodsX* 5 (2018) 599–608.

[20] Z. Bednarikova, M. Kubovcikova, I. Antal, A. Antosova, M. Gancar, J. Kovac, R. Sobotova, V. Girman, D. Fedunova, M. Koneracka, Z. Gazova, V. Zavisova, Silica-magnetite nanoparticles: synthesis, characterization and nucleic acid separation potential, *Surf. Interfaces* 39 (2023) 102942.

[21] S. Khizar, A.A. Al-Dossary, N. Zine, N. Jaffrezic-Renault, A. Errachid, A. Elaissari, Contribution of magnetic particles in molecular diagnosis of human viruses, *Talanta* 241 (2022) 123243.

[22] P. Voparilová, Z. Šplíchal, P. Švec, P. Kulich, O. Malina, M. Otyepka, O. Zítka, J. Kudr, Amine-modified magnetic particles: an efficient tool for enhanced RNA extraction, *Sep. Purif. Technol.* 356 (2025) 129788.

[23] A. Zelenáková, V. Zelenák, E. Benová, B. Kočíková, N. Király, P. Hrubovčák, J. Szűcsová, L. Nagy, M. Klementová, J. Mačák, V. Závišová, J. Bednářčík, J. Kupčík, A. Jacková, D. Volavka, J. Kosuth, Š. Vilček, The surface modification of the silica-coated magnetic nanoparticles and their application in molecular diagnostics of virus infection, *Sci. Rep.* 14 (2024) 14427.

[24] S. Berensmeier, Magnetic particles for the separation and purification of nucleic acids, *Appl. Microbiol. Biotechnol.* 73 (2006) 495–504.

[25] Y. Wang, Y.Y. Huang, Y.Q. Peng, Q.L. Cao, W.K. Liu, Z.C. Zhou, G.X. Xu, L. Li, R. Zhou, Development and validation of a rapid five-minute nucleic acid extraction method for respiratory viruses, *Virology J.* 21 (2024).

[26] J. Estelrich, E. Escribano, J. Queralt, M.A. Busquets, Iron oxide nanoparticles for magnetically-guided and magnetically-responsive drug delivery, *Int J. Mol. Sci.* 16 (2015) 8070–8101.

[27] L.T. Kuhn, A. Bojesen, L. Timmermann, M.M. Nielsen, S. Mørup, Structural and magnetic properties of core-shell iron–iron oxide nanoparticles, *J. Phys. Condens. Matter* 14 (2002) 13551.

[28] A.P. Tiwari, R.K. Satvekar, S.S. Rohiwal, V.A. Karande, A.V. Raut, P.G. Patil, P. B. Shete, S.J. Ghosh, S.H. Pawar, Magneto-separation of genomic deoxyribose nucleic acid using pH responsive Fe_3O_4 @silica@chitosan nanoparticles in biological samples, *RSC Adv.* 5 (2015) 8463–8470.

[29] Z.C. Zhang, Y. Cui, Q.H. Wan, Surface modification of magnetic silica microspheres and its application to the isolation of plant genomic nucleic acids, *Chin. J. Anal. Chem.* 35 (2007) 31–36.

[30] S. Mirna Lorena, P.C. Cynthia, A.R. Maria Isabela, V.M. Pamela, R.H. Gabriela, B. Jorge, G. Mariano, Nucleic acids isolation for molecular diagnostics: present and future of the silica-based DNA/RNA purification technologies, *Sep. Purif. Rev.* 52 (2023) 193–204.

[31] N. Capriotti, L.C.A. Morales, E. de Sousa, L. Juncal, M.L. Pidre, L. Traverso, M. F. López, M.L. Ferelli, G. Lavorato, C. Lillo, O.V. Robaina, N. Mele, C. Vericat, P. Schiardi, A.F. Cabrera, S. Stewart, M.H. Fonticelli, P.M. Zéliz, S. Ons, V. Romanowski, C.R. Torres, Silica-coated magnetic particles for efficient RNA extraction for SARS-CoV-2 detection, *Helijon* 10 (2024).

[32] A.D. Prasetya, M. Muflikhah, W.Z. Lubis, A. Insani, G.T. Sulungbudi, M. Mujamilah, U. Saepullah, Development of magnetic-silica particles and in-house buffers kit for SARS-CoV-2 and CDV RNA extraction, *Indonesian J. Chem.* 24 (2024) 81–93.

[33] S. Mikutis, G.J.L. Bernardes, Technologies for targeted RNA degradation and induced RNA decay, *Chem. Rev.* 124 (2024) 13301–13330.

[34] A. Nouvel, J. Laget, F. Duranton, J. Leroy, C. Desmetz, M.-D. Servais, N. de Préville, F. Galtier, D. Nocca, N. Builles, S. Rebuffat, A.-D. Lajoix, Optimization of RNA extraction methods from human metabolic tissue samples of the COMET biobank, *Sci. Rep.* 11 (2021) 20975.

[35] A.G. Díez, M. Rincón-Iglesias, S. Lanceros-Méndez, J. Reguera, E. Lizundia, Multicomponent magnetic nanoparticle engineering: the role of structure-property relationship in advanced applications, *Mater. Today Chem.* 26 (2022) 101220.

[36] B.D. Plouffe, S.K. Murthy, L.H. Lewis, Fundamentals and application of magnetic particles in cell isolation and enrichment: a review, *Rep. Prog. Phys.* 78 (2015) 016601.

[37] Y. Fu, T. Liu, H. Wang, Z. Wang, L. Hou, J. Jiang, T. Xu, Applications of nanomaterial technology in biosensing, *J. Sci. Adv. Mater. Devices* 9 (2024) 100694.

[38] T. Sugimoto, E. Matijević, Formation of uniform spherical magnetite particles by crystallization from ferrous hydroxide gels, *J. Colloid Interface Sci.* 74 (1980) 227–243.

[39] H. Cui, W. Ren, P. Lin, Y. Liu, Structure control synthesis of iron oxide polymorph nanoparticles through an epoxide precipitation route, *J. Exp. Nanosci.* 8 (2013) 869–875.

[40] W. Stöber, A. Fink, E. Bohn, Controlled growth of monodisperse silica spheres in the micron size range, *J. Colloid Interface Sci.* 26 (1968) 62–69.

[41] O. Malay, I. Yilgor, Y.Z. Menceloglu, Effects of solvent on TEOS hydrolysis kinetics and silica particle size under basic conditions, *J. Sol. Gel Sci. Technol.* 67 (2013) 351–361.

[42] P. Xu, H. Wang, R. Tong, Q. Du, W. Zhong, Preparation and morphology of SiO_2 /PMMA nanohybrids by microemulsion polymerization, *Colloid Polym. Sci.* 284 (2006) 755–762.

[43] S. Wurtzer, M. Duvivier, H. Accrombessi, M. Levert, E. Richard, L. Moulin, Assessing RNA integrity by digital RT-PCR: influence of extraction, storage, and matrices, *Biol. Methods Protoc.* 9 (2024).

[44] E. Hernán, J. Isasi, M. Rapp, M.A. Palafox, J.F. Marco, A structural, magnetic and colloidal stability study of uncoated and silica coated iron oxide samples prepared in two different surfactants, *J. Alloy. Compd.* 1009 (2024).

[45] R. Rani, P. Malik, S. Dhania, T.K. Mukherjee, Recent advances in mesoporous silica nanoparticle-mediated drug delivery for breast cancer treatment, *Pharmaceutics* 15 (2023).

[46] S. Ganguly, S. Margel, Magnetic polymeric conduits in biomedical applications, *Micromachines* 16 (2025).

[47] A.S. Picco, L.F. Ferreira, M.S. Liberato, G.B. Mondo, M.B. Cardoso, Freeze-drying of silica nanoparticles: redispersibility toward nanomedicine applications, *Nanomedicine* 13 (2018) 179–190.

[48] A. Almalik, I. Alradwan, M.A. Kalam, A. Alshamsan, Effect of cryoprotection on particle size stability and preservation of chitosan nanoparticles with and without hyaluronate or alginate coating, *Saudi Pharm. J.* 25 (2017) 861–867.

[49] G. Degobert, D. Aydin, Lyophilization of nanocapsules: instability sources, formulation and process parameters, *Pharmaceutics* 13 (2021).